Geometry Optimizations of the Ground and Excited Triplet State Structures of the Low-Valent Metal−Metal Bonded Isocyanide and Carbonyl Di- and Trinuclear Palladium Complexes Using Density Functional Theory

Réjean Provencher and Pierre D. Harvey*

Département de Chimie, Université de Sherbrooke, Sherbrooke (Québec), Canada J1K 2R1

Received June 24, 1995[⊗]

In relation to the known complexes $Pd_2(CNMe)_6^{2+}$ and $Pd_2(CN\text{-}t\text{-}Bu)_4Cl_2$, $Pd_2(tmb)_2Cl_2$ (tmb = 2,5-dimethyl-2′,5′-diisocyanohexane) and $Pd_3(dppm)_3CO^{2+}$ (dppm = $((C_6H_5)_2P)_2CH_2$), respectively, the ground and lowest energy triplet excited state geometries of the model compounds $Pd_2(CNMe)_4Cl_2$ and $Pd_2(CN(CH_2)_4NC)_2Cl_2$, and $Pd_3(PH_3)_6CO^{2+}$ have been optimized using density functional theory. The computations for ground state structures are in excellent agreement with the X-ray data. In the excited states, bond lengthening (due to the change in Pd−Pd bond order $0 \rightarrow 1$) is predicted. In the bridged species, $Pd_2(CN(CH_2)_4NC)_2Cl_2$, the computations reveal that twisting of the dihedral angle must occur in order to account for the large change in Pd−Pd distance. Finally, the Pd−Pd bond lengthening for the $Pd_3(dppm)_3CO^{2+}$ cluster in the $^3A_2$ excited state is predicted to be ∼0.19 Å relative to the ground state. This value has also been confirmed by an analysis of the emission band using Heller's time-dependent theory.

Introduction

The photoinduced homolytic bond cleavage of the low-valent Pd−Pd bond in binuclear complexes has been investigated by a number of research groups for some time now.[1,2] This photoprocess occurs in the triplet states[3] where a metal−metal (M−M) bond lengthening results from M−M antibonding interactions. The change in M−M bond length[4,5] in the excited states strongly depends upon the nature of the complexes and the extent of excited state mixing.[6] Recently, our group has been interested in the photochemical behavior of a trinuclear cyclic cluster, $Pd_3(dppm)_3CO^{2+}$ (dppm = $((C_6H_5)_2P)_2CH_2$), which photooxidatively break down to the monomeric Pd(dppm)Cl_2 complex (among other products) in the presence of chlorocarbons[7a] or photoadds O_2 using appropriate irradiation wavelengths and temperature conditions.[7b] On the basis of theoretical calculations (extended Hückel molecular orbital, EHMO), the M−M interactions are antibonding in the excited states,[8] which subsequently were confirmed experimentally.[9] We now report the results of our ground and triplet excited state geometry optimization calculations using density functional theory on three complexes $Pd_2(CN\text{-}t\text{-}Bu)_4Cl_2$, $Pd_2(tmb)_2Cl_2$ (tmb = 2,5-dimethyl-2′,5′-diisocyanohexane), and $Pd_3(dppm)_3CO^{2+}$. Bond lengthening is indeed predicted, but ligand structural deformation also occurs. For $Pd_3(dppm)_3CO^{2+}$, the computational results have important implications on its guest−host chemistry[7b,9] and, therefore, its photoreactivity.

Computational Details

The reported density functional calculations were all carried out utilizing the Amsterdam density functional (ADF) program, which was developed by Baerends *et al.*[10,11] and vectorized by Raveneck.[12] The numerical integration procedure applied for the calculations was developed by te Velde *et al.*[13] The geometry optimization procedure was based on the method developed by Versluis and Ziegler.[14] The electronic configurations of the molecular systems were described by an uncontracted double-ζ basis set[15] on palladium for 4s, 4p, and 5s and triple-ζ for 5d. Double- ζ STO basis sets[16] were used for phosphorous (3s, 3p), oxygen (2s, 2p), carbon (2s, 2p), nitrogen (2s, 2p), and hydrogen (1s), augmented with a single 4d polarization function for P, a single 3d one for O, C, and N, and a 2p function for H. No

[⊗] Abstract published in *Advance ACS Abstracts,* March 1, 1996.

(1) (a) Lemke, F. R.; Granger, R. M.; Morgenstern, D. A.; Kubiak, C. P. *J. Am. Chem. Soc.* **1990**, *112*, 4052. (b) Metcalf, P. S.; Kubiak, C. P. *J. Am. Chem. Soc.* **1986**, *108*, 4682. (c) Reinking, M. K.; Kullberg, M. L.; Cutler, A. R.; Kubiak, C. P. *J. Am. Chem. Soc.* **1985**, *107*, 3517. (d) Yamamoto, Y.; Yamazaki, H. *Bull. Chem. Soc. Jpn.* **1985**, *58*, 1843. (e) Perreault, D.; Drouin, M.; Michel, A.; Harvey, P. D. *Inorg. Chem.* **1992**, *31*, 2740. (f) Harvey, P. D.; Murtaza, Z. *Inorg. Chem.* **1993**, *32*, 4721.

(2) Reviews including this topic are also available: (a) Meyer, T. J.; Caspar, J. V. *Chem. Rev.* **1985**, *85*, 187. (b) Harvey, P. D. *J. Cluster Sci.* **1993**, *4*, 377.

(3) (a) Geoffroy, G. L.; Wrighton, M. S. *Organometallic Photochemistry*; Academic Press: New York, 1979. (b) Roundhill, D. M. *Photochemistry and Photophysics of Metal Complexes*; Plenum Press: New York, 1994.

(4) Miskowski, V. M.; Smith, T. P.; Loehr, T. M.; Gray, H. B. *J. Am. Chem. Soc.* **1985**, *107* , 7925.

(5) (a) Miskowski, V. M.; Rice, S. F.; Gray, H. B.; Dallinger, R. F.; Milder, S. J.; Hill, M. G.; Exstrom, C. L.; Mann, K. R. *Inorg. Chem.* **1994**, *33*, 1799. (b) Che, C.-M.; Butler, L. G.; Gray, H. B.; Crooks, R. M.; Woodruff, W. H. *J. Am. Chem. Soc.* **1983**, *105*, 5492.

(6) Harvey, P. D.; Dallinger, R. F.; Woodruff, W. H.; Gray, H. B. *Inorg. Chem.* **1989**, *28*, 3057.

(7) (a) Harvey, P. D.; Provencher, R.; Gagnon, J.; Zhang, T.; Fortin, D.; Hierso, K.; Drouin, M.; Socol, S. M. Submitted for publication. (b) Harvey, P. D.; Crozet, M.; Aye, K. T. *Can. J. Chem.* **1995**, *73*, 123.

(8) Harvey, P. D.; Provencher, R. *Inorg. Chem.* **1993**, *32*, 61.

(9) Harvey, P. D.; Hubig, S. M.; Ziegler, T. *Inorg. Chem,* **1994**, *33*, 3700.

(10) Baerends, E. J.; Ellis, D. E.; Ros, P. *Chem. Phys.* **1973**, *2* , 41.

(11) Baerends, R. J. Ph.D. Thesis, Vrije Universiteit, Amsterdam, 1975.

(12) Raveneck, W. In *Algorithms and Applications on Vector and Parallel Computers*; Rigie, H. J. J., Dekkor, Th. J., van de Vorst, H. A., Eds.; Elsevier: Amsterdam, 1987.

(13) Boerrigter, P. M.; te Velde, G.; Baerends, E. J. *Int. J. Quantum Chem.* **1988**, *33*, 87.

(14) Versluis, L.; Ziegler, T. *J. Chem. Phys.* **1988**, *88*, 322.

(15) (a) Snijders, G. J.; Baerends, E. J.; Vernooys, P. *At. Nucl. Data Tables* **1982**, *26*, 483. (b) Vernooys, P.; Snijders, G. J.; Baerends, E. *Journal of International Slater Type Basis Functions for the Whole Periodic System*; International Report; Free University of Amsterdam: Amsterdam, 1981.

(16) (a) Noodleman, L.; Norman, J. G. *J. Chem. Phys.* **1979**, *70*, 4903. (b) Noodleman, L. *J. Chem. Phys.* **1981**, *74*, 5737. (c) Noodleman, L.; Baerends, E. J. *J. Am. Chem. Soc.* **1984**, *106*, 2316.

0020-1669/96/1335-2113$12.00/0

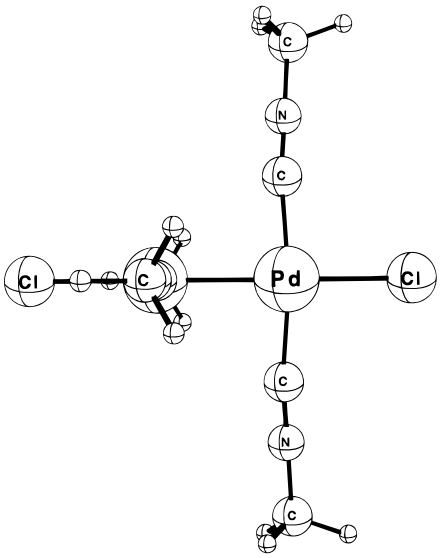

Figure 1. Optimized geometry for the model compound $Pd_2(CNMe)_4Cl_2$ in the ground state. The computations were restricted to D_{2d} geometry.

polarization function was used for palladium. The $1s^2\ 2s^2\ 2p^6\ 3s^2\ 3d^{10}$ configuration on palladium, the $1s^2\ 2s^2$ configuration on phosphorous, and the $1s^2$ configurations on oxygen, carbon, and nitrogen were treated by the frozen-core approximation.[11] A set of auxiliary[17] s, p, d, f, and g STO functions, centered on all nuclei, was used in order to fit the molecular density and present Coulomb and exchange potentials accurately in each self-consistent field (SCF) cycle. Energy differences were calculated by including the local exchange-correlation potential by Vosko *et al.*[18a] No nonlocal exchange and correlation corrections were made for the geometry optimizations. The emission spectra were analyzed using Heller's time-dependent theory,[18b] which gives results equivalent to those of a traditional Franck−Condon analysis.

Results and Discussion

Ground State. The first two complexes considered are $Pd_2(CN\text{-}t\text{-}Bu)_4Cl_2$[1d] and the closely related unbridged $Pd_2(CNMe)_6^{2+}$ dimer.[19] On the basis of the X-ray crystallographic results,[1d,19] one can easily consider the approximate molecular symmetry to be D_{2d} as the C−Pd−Pd−C dihedral angles are 82.7° for $Pd_2(CN\text{-}t\text{-}Bu)_4Cl_2$ [1d] and 86.4° for $Pd_2(CNMe)_6^{2+}$.[19] Solid state stacking may be at the origin of the deviation from 90°. For the computations, the model compound $Pd_2(CNMe)_4Cl_2$ was used in order to reduce the computation time, and the calculations were restricted to D_{2d} and C_{2v} symmetry. The C_{2v} symmetry was selected in order to give some degree of freedom to the ligands to adopt different configurations. The starting geometry was a structure where all angles were either 90 or 180°, and the bond distances were chosen close to the published values for $Pd_2(CN\text{-}t\text{-}Bu)_4Cl_2$ and $Pd_2(CNMe)_6^{2+}$, in order to reduce the number of iterative cycles. After the computations some minor distortions from the starting geometry were noticed (Figure 1 and Table 1). First of all, for C_{2v} symmetry, there is practically no difference between the different bond lengths and bond angles. The differences in the calculated bond distances and angles was less than 0.001 Å and 0.07°, respectively. Essentially, the C_{2v} optimized geometry has D_{2d} symmetry. Secondly, the comparison between the D_{2d} and C_{2v} optimized ground state geometries (bond distances and angles) is excellent. Finally, the comparison between the computed structures and the X-ray data is also excellent, including the deviation of the C−Pd−C unit away from linearity (computed, ∠CPdC = 174°; experimental, ∠CPdC = 170°). The most important data for this work are the Pd−Pd and Pd−L bond lengths. The $r(Pd_2)$ average computed value is 2.530 Å, and this compares particularly well with the average experimental value of 2.532 Å. The calculated and experimental Pd−Cl bond lengths are a little different (∼2.36 vs 2.41 Å).

Table 1. Comparison of the Calculated and Experimental Structures in the Ground State for Unbridged Pd_2 Complexes[a]

	$Pd_2(CNMe)_4Cl_2$ calculated, D_{2d}	$Pd_2(CN\text{-}t\text{-}Bu)_4Cl_2$ X-ray[1d]	$Pd_2(CNMe)_6^{2+}$ X-ray[19]
$r(Pd_2)$	2.523	2.532(2)	2.5310(9)
r(Pd−Cl)	2.361	2.410(7)	
r(Pd−C)	1.941	1.994(50)	1.963(5)
r(C≡N)	1.164	1.113(41)	1.139(3)
r(C−N)	1.388	1.472(22)	1.449(4)
∠CPdC	174.5	165.8	169.9(7)
∠PdCN	174.9	174.9	175.1(4)
∠CNC	178.8	166.8	178.3(5)
∠PdPdC	87.2	85.1	85.0(9)

[a] The X-ray data are averaged (angstrom units for bond distances and degrees for angles).

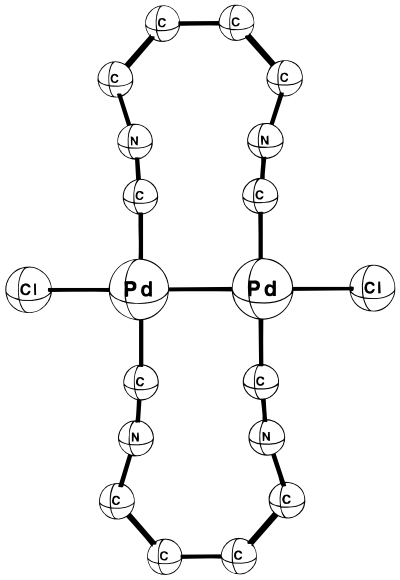

Figure 2. Optimized geometry for the model compound $Pd_2(CN(CH_2)_4NC)_2Cl_2$ in the ground state. The computations were restricted to D_{2h} symmetry. The H atoms are not shown.

The second molecule of interest is $Pd_2(tmb)_2Cl_2$. In order to reduce computation time, tmb was replaced by $CN(CH_2)_4NC$ and the calculations were performed in restricted D_{2h} molecular symmetry (including the bridging ligand). A second reason for using D_{2h} symmetry is that one can study the effect of ring strain on the Pd−Pd bond. In a recent study of $Pd_2(dmb)_2X_2$ complexes (dmb = 1,8-diisocyano-*p*-menthane; X = Cl, Br),[1] stress in the Pd−Pd bond was invoked in order to explain the increase in photoinduced homolytic metal−metal bond cleavage quantum yield. In subsequent work,[1f] the estimated $r(Pd_2)$ values for these complexes were 2.72 ± 0.05 Å, representing long Pd−Pd bonds. The results of the computer geometry optimizations are presented in Figure 2 and correspond to the following data: $r(Pd_2)$ = 2.588 Å, r(Pd−Cl) = 2.350 Å, r(Pd−C) = 1.941 Å, r(C≡N) = 1.167 Å, r(C−N) = 1.387 Å, ∠CPdC = 178.4°, ∠PdCN = 172.9°, ∠CNC = 169.1°, and ∠PdPdC = 89.2°. The most astonishing result is the ∠PdPdC angle, which is near 90° despite the ring strain induced by the planar $-(CH_2)_4-$bridge and the steric repulsions of the isocya-

(17) Krijn, J.; Baerends, E. J. In *Fit Function in the HFS-Method*; Internal Report (in Dutch); Free University of Amsterdam: Amsterdam, 1984.
(18) (a) Vosko, S. D.; Wilk, L.; Nusair, M. *Can. J. Phys.* **1990**, *58*, 1200. (b) Heller, E. J. *Acc. Chem. Res.* **1981**, *14*, 368.
(19) Goldberg, S. Z.; Eisenberg, R. *Inorg. Chem.* **1976**, *15*, 535.

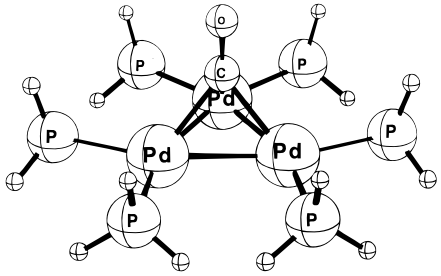

Figure 3. Optimized geometry for the model compound $Pd_3(PH_3)_6CO^{2+}$ in the ground state. The computations were performed in restricted C_{3v} geometry.

Table 2. Comparison of the Calculated and Experimental Structures in the Ground State for the Pd_3 Cluster

	$Pd_3(PH_3)CO^{2+}$ calcd	$Pd_3(dppm)_3CO^{2+}$ [a,b] X-ray
r(Pd−Pd)	2.592	2.604(30)
r(Pd−P)	2.317	2.318(30)
r(Pd−C)	2.080	2.105(17)
r(C═O)	1.170	1.165(5)
∠PdPdC	51.45	51.50
∠PdCPd	77.06	76.99
∠PdCO	134.0	133.70

[a] The X-ray data correspond to averaged values taken from ref 22 (*r* in angstroms, and angles in degrees). [b] The uncertainties in parentheses are the difference between the maximum and minimum data values observed.

nide carbons (the sum of the van der Waals radii is $1.67 \times 2 = 3.34$ Å).[20] This result clearly indicates that the square planar coordination is rather rigid and that the ring stress can only be released from a twisting around the Pd−Pd bond where the dihedral angle would be significantly greater than zero ($D_{2h} \rightarrow D_2$). The ring stress is felt in the ∠PdCN and ∠CNC angles which deviate from the linearity generally associated with the sp hybridation of the isocyanide C and N atoms. The calculated Pd−C, C≡N, and C−N bond lengths are not affected by the ring stress. The computed Pd−Pd bond distance has, however, increased from 2.532 to 2.588 Å (unbridged $D_{2d} \rightarrow$ bridged D_{2h}). This new value is far from the 2.72 ± 0.5 Å that was predicted from the spectroscopic findings[1f] but still is evidence for a ring stress effect on the Pd−Pd bond length. This value compares favorably with other Pd^{I}-Pd^{I} isocyanide complexes.[21]

The next complex investigated is the cluster $Pd_3(dppm)_3CO^{2+}$, which was treated using the model compound $Pd_3(PH_3)_6CO^{2+}$ under C_{3v} symmetry (Figure 3). The absence of the P−C−P bridge in the computations will determine the role of the dppm ligand in the Pd−Pd length, if any. The results (Table 2) show again excellent agreement between the calculations and the experimental data, including *r*(Pd−Pd). These results indicate that the dppm does not appear to induce any bond lengthening (despite the natural bite distance of ∼3.3 Å).

Excited States. The experimentally characterized lowest energy triplet excited states in the $Pd_2(dmb)_2X_2$ and $Pd_2(tmb)_2X_2$ complexes (X = Cl, Br) are the $^3(d\sigma d\sigma^*)$ states,[1f] where the Pd−Pd bond order is formally zero. Beside the Pd−Pd interactions, the Pd−L interactions also undergo some changes. Both in the LUMO and HOMO, the Pd−L interactions are antibonding according to the EHMO computations.[1f] In the

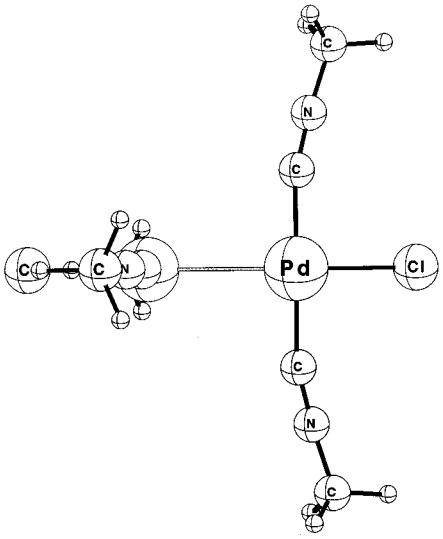

Figure 4. Optimized geometry for $Pd_2(CNMe)_4Cl_2$ in the $^3(d\sigma d\sigma^*)$ excited state.

Table 3. Comparison of the Calculated Structures of $Pd_2(CNMe)_4Cl_2$ in the Ground and Triplet $^3(d\sigma d\sigma^*)$ and $^3(d\pi^* d\sigma^*)$ Excited States[a]

	ground state	$^3(d\sigma d\sigma^*)$	$^3(d\pi^* d\sigma^*)$
r(Pd_2)	2.530	2.964	2.661
r(Pd−Cl)	2.366	2.405	2.424
r(Pd−C)	1.941	1.972	2.001
r(C≡N)	1.164	1.166	1.168
r(C−N)	1.388	1.387	1.388
∠CPdC	174.4	182.1	170.4
∠PdCN	174.9	167.8	171.4
∠CNC	179.2	176.7	177.1
∠PdPdC	87.2	91.0	85.2

[a] Distances in angstroms and angles in degrees.

LUMO, the atomic contribution of the donor atom is larger than in the HOMO (Chart 1).[1f] As a result, the Pd−L bonds should

Chart 1

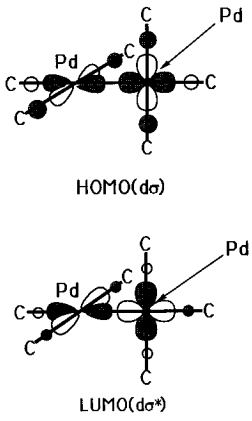

experience a slight lengthening in the $^3(d\sigma d\sigma^*)$ states,[1f] where the Pd−Pd bond order is formally zero. The calculations were first performed on the model compound $Pd_2(CNMe)_4Cl_2$ in D_{2d} symmetry (Figure 4, Table 3). Indeed slight increases in Pd−L bond lengths (∼+0.03 Å) have been computed in agreement with the EHMO predictions.[1f] The most striking feature in these computations is the drastic increase in Pd−Pd bond length (from 2.530 to 2.964 Å). At such a distance the Pd−Pd interactions are definitely weak, exceeding the distance found in pure Pd metal (2.777 Å). Interestingly, this value also compares favorably with the d^{10}−d^{10} $Pd_2(dppm)_3$ complex (*r*(Pd_2) =

(20) Cotton, F.; Wilkinson, G.; Gaus, P. L. *Basic Inorganic Chemistry*, 3rd ed.; Wiley: New York, 1995; p 61.
(21) See, for example: Yamamoto, Y.; Takahashi, K.; Yamazaki, H. *Chem. Lett.* **1985**, 201. *r*(Pd_2) = 2.56 Å.
(22) Provencher, R.; Aye, K. T.; Drouin, M.; Gagnon, J.; Boudreault, N.; Harvey, P. D. *Inorg. Chem.* **1994**, *33*, 3689.

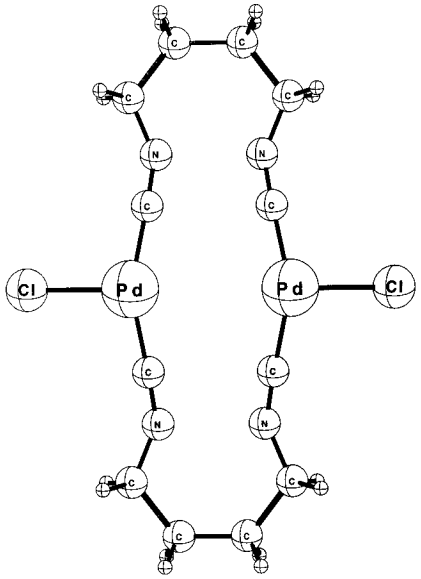

Figure 5. Optimized geometry for $Pd_2(CN(CH_2)_4NC)_2Cl_2$ in the $^3(d\sigma d\sigma^*)$ excited state.

2.956(1) Å), where no formal Pd−Pd bond occurs.[23] The *r*(C≡N) and *r*(C−N) distances remain virtually unaffected by the electronic excitation, as expected. The second observation is the large change in CPdC (from 174.4 to 182.1°) and PdCN angles (from 174.9 to 167.8°), indicating some kind of CNMe··· CNMe repulsions (Figure 4). The remaining bond angle data do not greatly change in this state.

The following set of geometry optimizations is focused on the T_2 state arising from an electronic excitation $d\pi^*$(HOMO-1) → $d\sigma^*$.[1f] The fact that both MO's are M−M antibonding implies that the Pd−Pd bond order should not change. However the $d_{yz}-d_{yz}$ and $d_{xz}-d_{xz}$ metal orbital overlaps are smaller than the $d_{z^2}-d_{z^2}$ interactions (for instance). As a consequence, the $d\pi^*$ orbital has a smaller M−M antibonding effect than the $d\sigma^*$. Under these conditions, a $d\pi^* \rightarrow d\sigma^*$ electronic excitation should lead to an excited state with a slightly longer Pd−Pd bond length. The geometry optimization was performed using the C_{2v} symmetry restriction. The results (Table 3) show that indeed *r*(Pd_2) increases to 2.661 Å (from 2.530 Å), but this bond length is still within the range of a Pd−Pd single bond.[1f] The M−L bond lengths (*r*(Pd−Cl), *r*(Pd−C)) also experience increases in this excited state, while *r*(C≡N) and *r*(C−N) are unaffected. The bond angles also remain close to the ground state values. There are very little differences between the bond distances and angles calculated for the same molecule under C_{2v} symmetry.

The computations on $Pd_2(CN(CH_2)_4NC)_2Cl_2$ in its $^3(d\sigma d\sigma^*)$ state under D_{2h} symmetry are interesting (Figure 5). First, a clear scission of the Pd−Pd bond occurs with *r*(Pd−Pd) now 3.697 Å. This cleavage is also accompanied by a noticeable molecular distortion within the ring. When the Pd−Pd bond vanishes, the ring strain distorts the CNC angle from 169.1° (ground state) to 146.1° in order to reestablish a more stable conformation in the NCC angle. As a consequence, the CNC angle deviates further from 180°, pushing the Pd−Cl groups outward, and the PdCN angle approaches linearity (177.9°). This unusual distortion is due to the fact that the computations restricted the molecule to D_{2h} symmetry. The Pd−Cl, Pd−C, C≡N, and N−C bond lengths are 2.363, 1.941, 1.203, and 1.428 Å, respectively. These distances are normal, except for *r*(N−C), which is longer than 1.388 Å (Table 1), and is associated with the planar $-(CH_2)_4-$ local ring stress imposed on the molecule. The main conclusions from these computations are that, firstly, in bridged species the Pd−Pd bond is also cleaved in the $^3(d\sigma d\sigma^*)$ state and secondly, twisting of the dihedral angle must occur to compensate for the change in Pd_2 distances.

Finally, the geometry optimization of the $Pd_3(PH_3)_6CO^{2+}$ model compound is considered. The LUMO, HOMO, and HOMO-1 are the a_2 , a_1, and e orbitals, respectively (Chart 2).[9]

Table 4. Comparison of the Calculated Structures of the Model Compound $Pd_3(PH_3)_6CO^{2+}$ in the Ground and Lowest Energy Triplet Excited States[a]

	$^1A_1$ (ground state)	$^3A_2$ (T1)	^3E (T_2)
r(Pd−Pd)	2.592	2.778	2.881
r(Pd−P)	2.317	2.376	2.339
r(Pd−C)	2.080	2.057	2.078
r(C═O)	1.170	1.169	1.168
∠PdPdC	51.45	47.54	46.10
∠PdCPd	77.06	84.91	87.79
∠PdCO	134.0	128.79	126.8l

[a] Bond lengths in angstroms and angles in degrees.

Chart 2

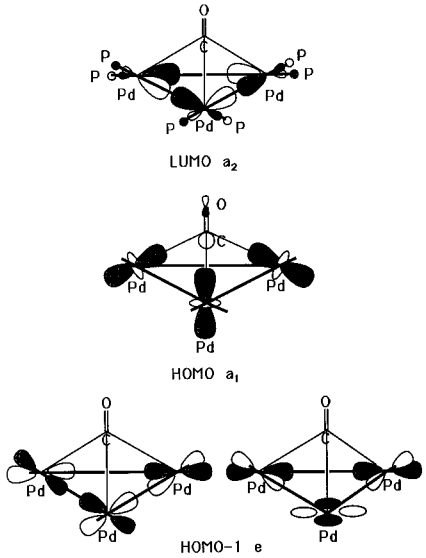

The two lowest energy triplet excited states are the $^3A_2$ and ^3E states ($^3A_2 < {}^3E$).[9] The LUMO and the HOMO-1 are formally Pd−Pd antibonding and bonding, respectively. The HOMO is only partially bonding, and, as a consequence, an excitation e → a_2 should generate excited states where the Pd···Pd interactions are weakened compared to the states generated by an a_1 → a_2 excitation. The optimization results for C_{3v} symmetry are presented in Table 4. The Pd−Pd bond length, as expected, increases in the excited states, and the relative order follows the EHMO predictions (Chart 2):$^1A_1 < {}^3A_2 < {}^3E$. The value of 2.881 Å corresponds to a distance where only weak Pd···Pd interactions occur. The 2.778 Å distance is also very long and is at the limit between a Pd−Pd single bond and a weak Pd··· Pd interaction.[24] The μ^3-CO bridging group may shorten the Pd···Pd distances here. The Pd−P bond lengths are also lengthened in these excited states, in agreement with the antibonding Pd−P character of the LUMO (Chart 2). For the Pd−C bonds, no significant change is computed in the ^3E state, consistent with C atomic contributions in the HOMO-1 and LUMO, but a slight decrease in length is found for the $^3A_2$ state. In the latter case, the excitation involved removing an electron

(23) Kirss, R. V.; Eisenberg, R. *Inorg. Chem.* **1989**, *28*, 3372.

(24) See data for Pd_2 and Pd_3 systems in: Perreault, D.; Drouin, M.; Michel, A.; Harvey, P. D. *Inorg. Chem.* **1993**, *32*, 1903.

from an antibonding Pd−C orbital (a_1) and placing it in the LUMO which is only localized in the Pd_3P_6 framework. Finally, the C═O group has essentially little or no role in these excitations, therefore, the bond length remains unaffected.

In order to address the role of the dppm bridging ligand on the Pd−Pd bond length in $Pd_3(dppm)_3CO^{2+}$, the P···P distances are examined. In the ground state, this separation is 3.257 Å, while, in the $^3A_2$ and ^3E excited states, these distances are 3.396 and 3.901 Å, respectively. With a natural bite distance of 3.3 Å, the dppm ligand does not impose any significant Pd−Pd−P−C−P ring stress on the Pd−Pd interactions in the ground and $^3A_2$ states. For the ^3E state, the larger 3.9 Å P···P distance indicates that the dppm ligand (∼3.3 Å) decreases slightly the Pd···Pd separation.

Excited State Distortion. The excited state distortion in the $^3A_2$ (T_1) state of $Pd_3(PH_3)_6CO^{2+}$, ΔQ, is ∼0.186 Å according to the computed ground and excited state Pd−Pd distances. There is no Pd−Pd bond distance evaluated experimentally for $Pd_3(dppm)_3CO^{2+}$ in the $^3A_2$ state. In order to address experimentally the Pd−Pd bond distance in the excited state, the phosphorescence spectrum of $Pd_3(dppm)_3CO^{2+}$ has been analyzed using Heller's time-dependent theory which is equivalent to a traditional Franck−Condon analysis. The time-dependent formulation of Heller's theory applied to electronic spectroscopy, involves the use of wavefunctions which include both the electronic transition moment between two Born−Oppenheimer potential surfaces and the ground-state vibrational wave functions. For absorption spectra, the wave functions are displaced in the wave packet and evolve with time acording to the time-dependent Schrödinger equation. The overlap between the wave functions at $t = 0$ and at $t = t$ is Fourier transformed in order to give the spectrum. Since the emission band of $Pd_3(dppm)_3CO^{2+}$ is vibrationally unstructured, a number of assumptions must be employed. In previous works on the d^9-d^9 $Pd_2(dmb)_2X_2$ complexes (X = Cl, Br), a first and second moment band analysis demonstrated that only one vibrational mode ($\nu(Pd_2)$) could describe adequately the temperature dependence of ν_{max} (first moment) and the bandwidth at half-maximum (fwhm: second moment) of the $d\sigma \rightarrow d\sigma^*$ absorption band.[1f] In a subsequent study on $Pd_3(dppm)_3CO^{2+}$, the first and second moment band analysis demonstrated that a minimum of two ground state vibrational modes were necessary to appropriately describe the temperature dependence of ν_{max} and fwhm of the $^1E \leftarrow {}^1A$ absorption bands.[9] Both ν_{max} and fwhm are related to the relative "hot band" populations. These modes ended up being both the a_1 and e $\nu(Pd_2)$ modes (i.e., 204 and 143 cm^{-1}, respectively, as observed from Raman spectroscopy).[9] For the emission band, it is also assumed that the Franck−Condon active vibrational modes are the a_1 and e $\nu(Pd_2)$ modes. In the fitting procedure, Heller's theory involved the adjustment of five parameters: position of the 0−0 component, $\nu(Pd_2)$ a_1 (ground state), $\nu(Pd_2)$ e (ground state), Δ, (unitless) for $\nu(Pd_2)$ a_1, and Δ for $\nu(Pd_2)$ e. The other parameters (Γ) and vibrational bandwidth) were kept normal (1×10^{-12} s, 400 cm^{-1}, respectively). By fixing $\nu(Pd_2)$ a_1 and $\nu(Pd_2)$ e at 204 and 143 cm^{-1}, only three parameters were left adjustable. During the fitting procedures, the quality of the fit turned out to be very sensitive to the changes in the adjustable parameters. Also, Δ for $\nu(Pd_2)$ a_1 and e were found to be interdependent: the fwhm did not change when Δ for $\nu(Pd_2)$ a_1 was increased by the amount by which Δ for $\nu(Pd_2)$ e was decreased. This dependence is due to the fact that Heller's model imposes equal intensity to all vibrational modes involved in the calculations. This is in reality rarely the case. The results obtained from these computations are considered approximate, and the ΔQ obtained for the a_1 and e $\nu(Pd_2)$ modes are averaged in order to obtain a more reliable value. The best fit was obtained for 0−0 = 15 670 cm^{-1}, Δ for $\nu(Pd_2)$ $a_1 = 5.45$, and Δ for $\nu(Pd_2)$ e = 4.30 (Figure 6). The position of the 0−0 is close to that previously calculated by Ziegler *et al.* (15 938 cm^{-1}) for the corresponding absorption.[9] The ΔQ obtained for the two modes are 0.172 and 0.199 Å,[25] respectively, averaging ∼0.186 Å. The comparison between this value and the computed ADF prediction is obviously excellent, but given the number of approximations made, the uncertainty is expected to be large.

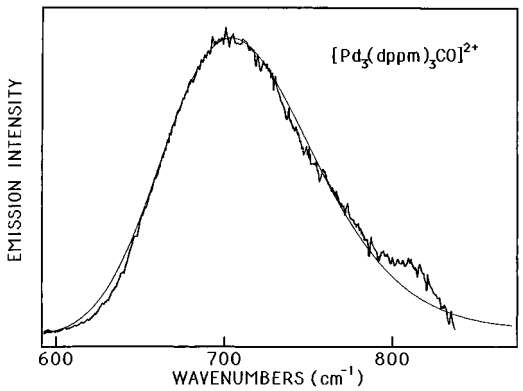

Figure 6. Comparison of the experimental (ref 8; broken line) and calculated (smooth line) emission spectrum of $Pd_3(dppm)_3CO^{2+}$ in solution at 77 K.

A similar analysis was performed on the emission spectrum of $Pt_3(dppm)_3CO^{2+}$ (λ_{max} = 625 nm).[9] The results are as follows: 0−0 = 18 190 cm^{-1}, $\nu(Pt_2)$ a_1 = 149 cm^{-1}, [9] $\nu(Pt_2)$ e = 129 cm^{-1}, [9] Δ for $\nu(Pt_2)$ $a_1 = 9.5$, and Δ for $\nu(Pt_2)$ e = 8.1. The calculated ΔQ are 0.342 and 0.314 Å, averaging ∼0.33 Å. Hence, with an average ground state r(Pt−Pt) ∼2.63 Å,[26] the r(Pt−Pt) value in the emissive excited state is ∼2.96 Å. This value is a little shorter than that of $Pt_2(dppm)_3$ for which no formal Pt−Pt bond occurs ($r(Pt_2) = 3.025$ Å)[27] and indicates that some Pt···Pt interactions are still present.[28]

Final Comments

These results have an important implication on the guest−host chemistry of $Pd_3(dppm)_3CO^{2+}$ in the excited states. With an increase in Pd−Pd bond length, the cavity size should increase proportionally. In the $^3A_2$ state (T_1), this increase is on the order of ∼0.186 Å. This way, the cavity may become less selective toward substrate···Pd_3 center interactions. In order to design an unsaturated Pd_3 complex exhibiting a cavity similar to that of the $^3A_2$ state, one can modify the bridging ligand. By replacing P (covalent radii = 1.10 Å)[20] by As (covalent radii = 1.22 Å), i.e., dppm to dpam ($(C_6H_5)_2As)_2CH_2$), the phenyl··· phenyl separation (along the As−Pd−Pd−As axis) would

(25) The equation converting the unitless excited state distortion Δ into ΔQ (Å) is $\Delta Q = \{(Nh)/(m(2\pi)cv)\}^{1/2}(10^8\Delta)$, where N is the Avogadro number, c is the speed of light (3×10^{10} cm/s), h is the Planck constant, and m is the reduced mass adapted, for a triangular cluster. For the a_1 mode, m is considered to be the $Pd(P(C_6H_5)_2)_2$ fragment; $m = m[Pd(P(C_6H_5)_2)_2]/3$. For the e mode, m is taken as $m = m[Pd(P(C_6H_5)_2)]/2$. These assignments are made according to the nuclear displacements in relation to the fragments being involved in a_1 and e vibrational modes.

(26) Puddephatt, R. J.; Manojlovic-Muir, L.; Muir, K. W. *Polyhedron* **1990**, *9*, 2767.

(27) (a) Manojlovic-Muir, L. J.; Muir, K. W. *J. Chem. Soc., Chem. Commun.* **1982**, 1155. (b) Manojlovic-Muir, L.; Muir, K. W.; Grossel, M. C.; Brown, M. P.; Nelson, C. D.; Yavari, A.; Kallas, E.; Moulding, R. P.; Seddon, K. R. *J. Chem. Soc., Dalton Trans.* **1985**, 1955.

(28) Harvey, P. D.; Truong, K. D.; Aye, K. T.; Drouin, M.; Bandrauk, A. D. *Inorg. Chem.* **1994**, *33*, 2347.

increase by ~0.24 Å. In this way, density functional theory serves as a good molecular modeling device in directing further work on the understanding of the excited state behavior of organometallic clusters.

Acknowledgment. P.D.H. thanks the Natural Sciences and Engineering Research Council of Canada (NSERC) and the Fond concerté pour l'avancement de la recherche (FCAR) for operating grants and the government of Quebec (Affaires Internationales) for a travel grant to Calgary. R.P. is grateful to the Université de Sherbrooke for institutional scholarships. The authors acknowledge Professor Tom Ziegler and his research group (University Calgary) for introducing them to the ADF program and allowing the use of the computers in their laboratories and at the University of Calgary for some of the calculations presented in this work.

IC950761G